Role of histidine interruption in mitigating the pathological effects of long polyglutamine stretches in SCA1: A molecular approach

SOMDUTTA SEN, DEBASIS DASH, SANTOSH PASHA, AND SAMIR K. BRAHMACHARI

Functional Genomics Unit, Institute of Genomics & Integrative Biology (formerly Centre for Biochemical Technology), CSIR, Delhi-110007, India

(RECEIVED July 19, 2002; FINAL REVISION January 4, 2003; ACCEPTED January 16, 2003)

Abstract

Polyglutamine expansions, leading to aggregation, have been implicated in various neurodegenerative disorders. The range of repeats observed in normal individuals in most of these diseases is 19–36, whereas mutant proteins carry 40–81 repeats. In one such disorder, spinocerebellar ataxia (SCA1), it has been reported that certain individuals with expanded polyglutamine repeats in the disease range ($Q_{12}HQHQ_{12}HQHQ_{14/15}$) but with histidine interruptions were found to be phenotypically normal. To establish the role of histidine, a comparative study of conformational properties of model peptide sequences with ($Q_{12}HQHQ_{12}HQHQ_{12}$) and without (Q_{42}) interruptions is presented here. $Q_{12}HQHQ_{12}HQHQ_{12}$ displays greater solubility and lesser aggregation propensity compared to uninterrupted Q_{42} as well as much shorter Q_{22}. The solvent and temperature-driven conformational transitions (β structure ↔ random coil → α helix) displayed by these model polyQ stretches is also discussed in the present report. The study strengthens our earlier hypothesis of the importance of histidine interruptions in mitigating the pathogenicity of expanded polyglutamine tract at the SCA1 locus. The relatively lower propensity for aggregation observed in case of histidine interrupted stretches even in the disease range suggests that at a very low concentration, the protein aggregation in normal cells, is possibly not initiated at all or the disease onset is significantly delayed. Our present study also reveals that besides histidine interruption, proline interruption in polyglutamine stretches can lower their aggregation propensity.

Keywords: Aggregation; β-hairpin; circular dichroism; histidine interruption; polyglutamines; SCA1; TFE

There are at least nine neurodegenerative disorders that are caused by expanded CAG triplet repeats coding for variable length polyglutamine stretches (David et al. 1997; Cummings and Zoghbi 2000; Nakamura et al. 2001). Polyglutamine tract expansion is nonpathogenic up to a threshold length but larger expansions cause neurodegenerative diseases including different types of spinocerebellar ataxia, Huntington's disease (HD), spinobulbar muscular atrophy (Kennedy disease), and dentatorubralpallidoluysian atrophy (DRPLA). In all these cases the CAG repeat is located within the coding region and is translated into a stretch of polyglutamine residues. The range of repeats observed in normal individuals in most of these diseases is 19–36, whereas mutant proteins carry 40–81 repeats (Cummings and Zoghbi 2000). This expansion results in formation of intracellular deposits or aggregates in the neurons. The accepted view is that these depositions are pathogenic in nature and results in cell death and subsequent neurodegeneration (Davies et al. 1997; Martindale et al. 1998; Koo et

Reprint requests to: Samir K. Brahmachari, Institute of Genomics & Integrative Biology (formerly Centre for Biochemical Technology), CSIR, Mall Road, Delhi-110007, India; e-mail: skb@cbt.res.in; fax: 91-11-27667471.

Abbreviations: Q, glutamine; H, histidine; P, proline; Poly Q, polyglutamine; TFE, trifluoroethanol; HFIP, hexafluoroisopropanol; SSC buffer, sodium chloride/sodium citrate buffer, MALDI-ToF, matrix assisted laser desorption ionization-time of flight; HPLC, high performance liquid chromatography.

Symbols: α helix, alpha helix; β sheet, beta sheet.

Article and publication are at http://www.proteinscience.org/cgi/doi/10.1110/ps.0224403.

al. 1999). However, as of yet, the exact molecular mechanism underlying the pathogenesis of polyglutamine repeat disorders has not been satisfactorily ascertained.

The glutamine stretch in all the diseases caused by polyglutamine expansions is encoded by the CAG codon (Chung et al. 1993). In case of one of the disease loci, spinocerebellar ataxia type1 (SCA1), the abnormalities is the result of a highly polymorphic CAG repeat stretch in the SCA1 gene located on chromosome 6p23 (Orr et al. 1993). The repeat stretch codes for a polyglutamine repeat that resides in the amino-terminal half of the SCA1 protein. Most of the normal proteins (93%) in SCA1 carry glutamine repeats interrupted by 1–2 histidine residues with a configuration of the type $(Q)_n$-H-Q-H-$(Q)_n$. However, mutant proteins contain a pure stretch of uninterrupted CAG trinucleotide that range from 39–82 repeats (Chung et al. 1993).

The conformation of polyglutamines has been a matter of debate for quite some time and currently is a focus of intense studies. Polyglutamines were reported to form β sheets strongly held together by hydrogen bonds (Perutz et al. 1994; Kelly 1998; Sharma et al. 1999). On the basis of model peptides, random coil conformation of polyglutamines in soluble monomeric form was also proposed by different groups (Altschuler et al. 1997; Chen et al. 2001). Recently, it has been demonstrated that polyglutamine aggregates have amyloid-like features exhibiting β sheet-rich conformation (Chen et al. 2002).

Our earlier studies (Sharma et al. 1999; Brahmachari et al. 2000) based on model peptides, demonstrated the effect of substitution of histidine residues in short polyglutamine stretches (Q_8HQHQ_8, $Q_{10}HQHQ_{10}$, $Q_8HQ_4HQ_8$, Q_{22}). We showed that polyglutamine tracts with histidine interruptions as observed in the normal SCA1 sequences, have relatively higher solubility and possess less aggregation propensity as compared to uninterrupted continuous stretches. This study provided evidence about how a point mutation with a change in amino acids could modulate the conformational properties that might be responsible for the onset of the disease processes.

Our present study is primarily focused on two separate reports (Quan et al. 1995; Calabresi et al. 2001) that described individuals with 44 repeats and 45 repeats, respectively, in the SCA1 protein. Although the repeat length was well within the disease range for SCA1, the individuals were found to be phenotypically normal. On sequencing it was found that the glutamine repeat was interrupted twice by an HQH motif, to yield a configuration of the type $Q_{12}HQHQ_{12}HQHQ_{14/15}$. Our work is mainly aimed at studying the conformational properties of a very similar sequence $Q_{12}HQHQ_{12}HQHQ_{12}$ to determine how the intermediate histidine substitution aids in mitigating the pathogenicity of expanded poly Q stretch.

Our study suggests that histidine interruptions play a dominant role in enhancing the solubility and decreasing the aggregation propensity of long polyglutamine stretches, which in turn might be responsible for lowered pathogenicity of expanded poly Q tract at the SCA1 locus. The work further shows that not only histidine interruptions, but even proline incorporation in model peptides can substantially reduce the aggregation propensities of continuous stretches. Furthermore, the study demonstrates the solvent- and temperature-dependent conformational transitions of polyglutamines with and without histidine interruptions.

It is relevant to mention here that most of the previous studies related to biophysical characterization of polyglutamine stretches, have been carried out using peptide sequences flanked by other amino acids (lysine, aspartic acid) to tackle the problem of insolubility. However, because our present study is mainly focused on a biologically relevant sequence observed in the actual protein, we have strictly adhered to a similar peptide sequence without any flanking residues. Furthermore, the problem of insolubility and aim of studying the peptide in the monomeric state has been satisfactorily handled by adopting the recently developed method of disaggregation of polyglutamines (Chen and Wetzel 2001). Thus, we have succeeded in studying the conformation of various peptide sequences in both monomeric as well as aggregated forms, which could possibly explain the contrasting set of results obtained by various groups on the conformation of polyglutamines.

Results

Biophysical characterization of a series of peptides with special emphasis on $Q_{12}HQHQ_{12}HQHQ_{12}$ and the corresponding uninterrupted stretch Q_{42} was carried out. The results obtained from other smaller sequences (Q_{22}, Q_8HQHQ_8) have also been discussed to stress the importance of length on solubility and aggregation propensity. The peptides obtained followed by their synthesis and subsequent high performance liquid chromatography (HPLC) purification were not in their completely disaggregated and monomeric form as observed by scattering and HPLC studies. Thus, it was found essential to study the conformation of model peptides both in the aggregated as well as in the monomeric (disaggregated) states.

Conformational study of aggregated peptides in aqueous buffer

The circular dichroism (CD) profile of histidine interrupted $Q_{12}HQHQ_{12}HQHQ_{12}$ (before disaggregation) at all measured concentrations in sodium chloride/sodium citrate buffer at pH 7.2 exhibited a positive band at 196 nm and a negative band ~220 nm (Fig. 1A). On the other hand, Q_{42} (without His interruptions) displayed a positive band at 202 nm and a negative band ~222 nm (Fig. 1B). Both the spectra were indicative of a β secondary structure. The position of

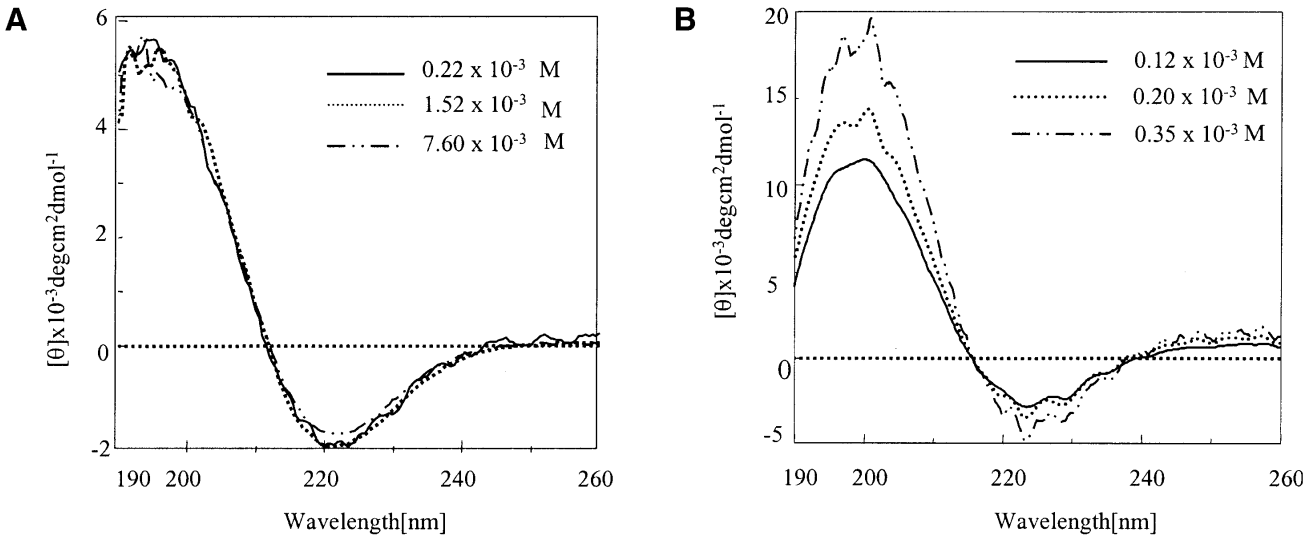

Figure 1. CD spectra of HPLC-purified $Q_{12}HQHQ_{12}HQHQ_{12}$ and Q_{42} in sodium chloride/sodium citrate buffer at various concentrations. (*A*) $Q_{12}HQHQ_{12}HQHQ_{12}$ exhibits a concentration-independent CD pattern indicating intramolecular nature of the β structure. (*B*) Q_{42} shows a concentration-dependent CD pattern, indicating stabilization of the β structure through intermolecular hydrogen bonding.

π–π^* and n–π^* transitions for Q_{42} at 202 and 222 nm, respectively, indicated a tightly linked and wide intermolecular β-sheet structure. The highly intermolecular nature of the structure was further indicated by the concentration-dependent CD profile. In contrast $Q_{12}HQHQ_{12}HQHQ_{12}$ displayed a concentration-independent CD pattern indicating intramolecular nature of the β structure (Perutz et al. 1994). The blue shifted CD band in the region 195–196 suggested that β structure formed, which does not involve large number of strands and stabilization of the structure is mainly through intramolecular hydrogen bonding (Chothia 1973). The highly aggregating nature of Q_{42} was evident from the disturbed CD profile resulting from precipitation of the peptide at a relatively lower concentration range as compared to $Q_{12}HQHQ_{12}HQHQ_{12}$.

Conformational study of disaggregated peptides in aqueous buffer

The solubilization and disaggregation protocol reported using 1:1 trifluoroacetic acid (TFA) and hexafluoroisopropanol (HFIP) solvent mixture (Chen and Wetzel 2001) was adopted to disaggregate the peptides to make them readily soluble in aqueous buffers. It is relevant to mention here that larger polyglutamine stretches without histidine interruptions, especially Q_{42}, required longer time and greater number of treatments with TFA/HFIP to acquire them in completely disaggregated forms. Figure 2 displays the matrix assisted laser desorption ionization-time of flight (MALDI-ToF) profile of Q_{42} after disaggregation. The disaggregated peptides were further subjected to CD and Rayleigh scattering studies (to study propensity for aggregation). Figure 3 displays the CD profile of $Q_{12}HQHQ_{12}HQHQ_{12}$ and Q_{42} in disaggregated (monomeric) states. The CD profiles of all the disaggregated peptides (with or without histidine interruptions) at neutral pH displayed an unordered structure characterized by a minimum at 197 nm (Greenfield and Fasman 1969). Both spectra displayed an insignificant effect on the molar ellipticity with increasing the temperature, justifying the suggested unordered structure (data not shown).

Solubility of proline substituted polyglutamines

Our earlier work (Sharma et al. 1999; Brahmachari et al. 2000) on short histidine interrupted polyglutamine se-

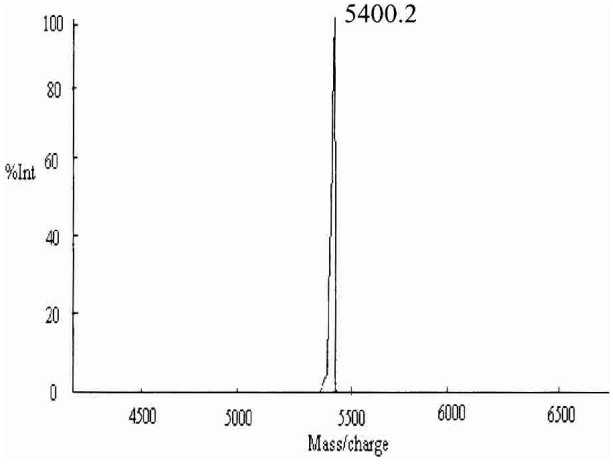

Figure 2. MALDI-ToF analysis in linear positive mode displays M^++1 peak at 5400.2 for Q_{42} after disaggregation with TFA/HFIP.

quences (Q_8HQHQ_8, $Q_{10}HQHQ_{10}$) showed that they have lower aggregation propensity as compared to Q_{22} (without interruption). To ascertain whether other amino acids of comparable structure could possibly exert a similar effect on the peptide solubility, histidine was replaced by proline in these sequences. The proline-incorporated peptides Q_8PQPQ_8 and Q_8HQPQ_8 were synthesized and subjected to complete disaggregation experiments as discussed above. The Rayleigh scattering experiments displayed even higher solubility and lower aggregation propensity of proline-substituted model peptides as compared to Q_8HQHQ_8 (data not shown) and their solubility pattern followed this trend $Q_8PQPQ_8 > Q_8HQPQ_8 > Q_8HQHQ_8 > Q_{22}$. The CD study of the disaggregated proline-incorporated peptides displayed an unordered structure with a minimum at 197 nm [data shown along with trifluoroethanol (TFE) dependence study of Q_8PQPQ_8; Fig. 6B]. Our work, based on model peptides, suggests that not only histidine interruptions, even proline interruptions, aid in slowing down the process of aggregation. The role of proline in enhancing the solubility of peptides was also reported in case of fragments of Alzheimer's peptide β /A4 (Wood et al. 1995).

Time-dependent conformational transitions

The peptides in their disaggregated states displayed widely different tendencies of aggregation with time. Figure 4 shows the time-dependent aggregation pattern (Rayleigh scattering) of Q_{42} and $Q_{12}HQHQ_{12}HQHQ_{12}$. We monitored the aggregation reactions following Rayleigh scattering (Chen et al. 2001) increases over time. In the same concentration range, Q_{42} displayed higher propensity for aggregation and

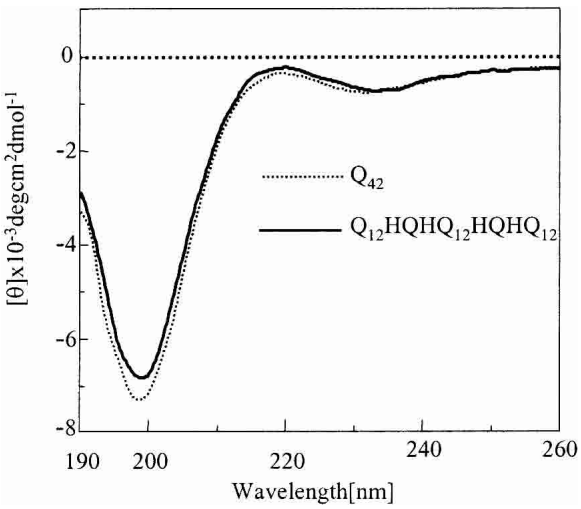

Figure 3. CD study of monomeric (disaggregated by TFA/HFIP) $Q_{12}HQHQ_{12}HQHQ_{12}$ and Q_{42}. CD data indicate unordered conformation for $Q_{12}HQHQ_{12}HQHQ_{12}$ (solid line) and Q_{42} (dotted line) with minimum at 197 nm indicative of an unordered structure.

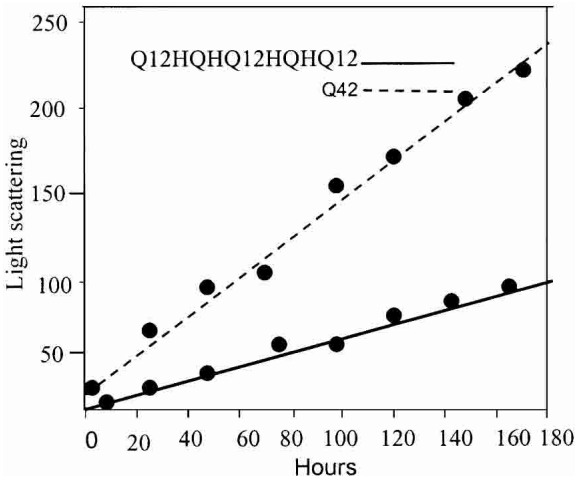

Figure 4. Time-dependent Rayleigh scattering study of disaggregated $Q_{12}HQHQ_{12}HQHQ_{12}$ (solid line) and Q_{42} (dotted line). Q_{42} displays much higher degree of scattering as compared to $Q_{12}HQHQ_{12}HQHQ_{12}$, suggesting higher aggregation potential of Q_{42}.

followed the trend of $Q_{42} > Q_{22} > Q_{12}HQHQ_{12}HQHQ_{12}$. The aggregation kinetics has been elaborately discussed in a recent article (Chen et al. 2001); we focused mainly on comparing the aggregation propensity of interrupted and continuous stretch polyglutamines.

In another set of experiments all these peptides (5×10^{-4} M, immediately after disaggregation) were monitored for their time-dependent conformational transitions on standing by circular dichroism. An aliquot of disaggregated peptides was left at room temperature and the CD profile was monitored over a period of 60 days and CD data were acquired after an interval of 10 days. The Table 1 displays the propensity for β structure adoption with time. Thus, Q_8HQHQ_8, Q_8PQPQ_8, and $Q_{12}HQHQ_{12}HQHQ_{12}$ retained the native unordered structure for a much longer period as compared to Q_{22} and Q_{42}. In fact, Q_{42} started showing visual signs of aggregation within 10–12 h of disaggregation. Correlation of these two data clearly suggest the greater propensity of continuous poly Q stretch to aggregate faster and acquire a β structure more promptly as compared to histidine interrupted analogs.

The fact that aggregated β-sheet structure adopted by polyglutamines with and without interruptions have similar conformational features have been recently reported (Calabresi et al. 2001) based on similar antibody-binding potential of both polyglutamine stretches. However, our findings based on CD and aggregation studies indicate that in spite of having similar structure they display widely different degrees of aggregation potential.

Solvent-dependent conformational transitions

We investigated the influence of various solvents like TFE, HFIP, and acetonitrile (CH_3CN) on the peptides under con-

Table 1. *Time-dependent conformational transition monitored by CD studies of Q_8HQHQ_8, $Q_{12}HQHQ_{12}HQHQ_{12}$, Q_{22}, Q_{42}, and Q_8PQPQ_8*

	Number of days					
Peptides	10	20	30	40	50	60
Q_8HQHQ_8	U.O	U.O	U.O	U.O	U.O	β
$Q_{12}HQHQ_{12}HQHQ_{12}$	U.O	U.O	U.O	β	β	β
Q_{22}	U.O	β	β	β	β	β
Q_{42}	β	β	β	β	β	β
Q_8PQPQ_8	U.O	U.O	U.O	U.O	U.O	U.O

U.O = unordered; β = β structure.
The experimental observations indicate that in the same concentration range Q_{42} and Q_{22} undergo a transition from unordered to β conformation in a relatively much shorter period of time as compared to $Q_{12}HQHQ_{12}HQHQ_{12}$.

sideration. The peptides studied here showed wide differences in their TFE dependence. Histidine interrupted polyglutamines (in β state, i.e., before disaggregation) of shorter length, e.g., Q_8HQHQ_8, displayed significant TFE dependence at lower concentration range (Brahmachari et al. 2000). However, poly Q peptides without histidine interruptions of similar (Q_{22}) or longer length (Q_{42}) displayed marginal or no effect with TFE. $Q_{12}HQHQ_{12}HQHQ_{12}$ exhibited strengthening of the positive band with increase in TFE percentage (Fig. 5), although the effect was more significant in case of Q_8HQHQ_8. Even for proline-incorporated peptides (Q_8HQPQ_8 or Q_8PQPQ_8) both bands at 196 nm and 220 nm showed higher intensity on enhancing the TFE concentration. Q_{42} left in TFE for a longer period also did not exhibit any noticeable change in molar ellipticity, however, it is worth mentioning that shorter histidine-interrupted peptides when left in TFE for days, displayed further increases in molar ellipticity.

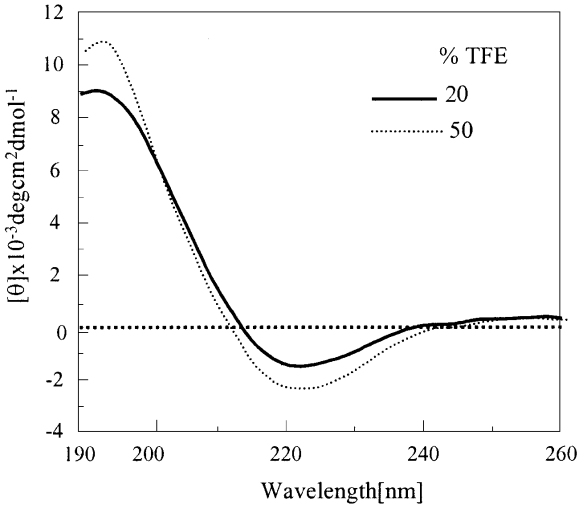

Figure 5. Effect of TFE on β structure of $Q_{12}HQHQ_{12}HQHQ_{12}$ shown at 20% (solid line) and 50% (dotted line) TFE. The increase in molar ellipticity with increase in TFE concentration indicates intramolecular nature of the β structure.

The effect of TFE on the disaggregated, unordered peptides was more profound, as demonstrated in Figure 6A, for $Q_{12}HQHQ_{12}HQHQ_{12}$. When incremental portions of TFE was added to peptide solution in buffer, a progressive shift from unordered to α-helical structure was observed, as displayed by peaks at 208 and 222 nm. $Q_{12}HQHQ_{12}HQHQ_{12}$ seemed to adopt a substantial α-helical conformation at 50% TFE concentration. In contrast, Q_{42} attained the same conformation at a much higher (65%) TFE percentage (data not shown). An isodichroic point at 202 nm, which indicated an equilibrium between two types of structures, namely random coil and α-helix (Woody 1995) was shown by all the peptides. This could be attributed to the weak proton-donating nature of TFE that facilitates intramolecular hydrogen bonding than intermolecular hydrogen bonding (Barrow et al. 1992; Sonnichsen et al. 1992; El-Agnaf et al. 1998). Thus, under conditions where α helix is in equilibrium with random structure, the former is stabilized in TFE. Proline-incorporated peptide Q_8PQPQ_8 also adopted α-helical conformation on adding TFE (Fig. 6B) with a significantly sharp minimum at 208 nm and an isodichroic point at 202 nm. The study in the presence of another helix-enhancing solvent HFIP also displayed similar results.

The peptides in helical state left in 50% TFE during a longer period of time displayed interesting results and the effect was prominent in case of continuous stretch. Q_{42} displayed lowering of the α-helical content (flattening of the valley at 208 nm) of the peptide indicated by decreased intensity of the 208-nm band, where intensity was found to be almost same as the 222-nm band. However, $Q_{12}HQHQ_{12}HQHQ_{12}$, along with Q_8HQHQ_8 and corresponding proline derivatives, did not display such transitions in the same time period (data not shown). Thus, Q_{42}, even in presence of TFE (50%), displayed greater tendency to aggregate into a β structure from α-helical conformation as compared to interrupted peptides. These data suggest that, although all these peptides have a tendency to adopt a helical structure from an unordered conformation in the presence of TFE, histidine-interrupted peptides adopt a helical conformation at lower TFE concentration and have the

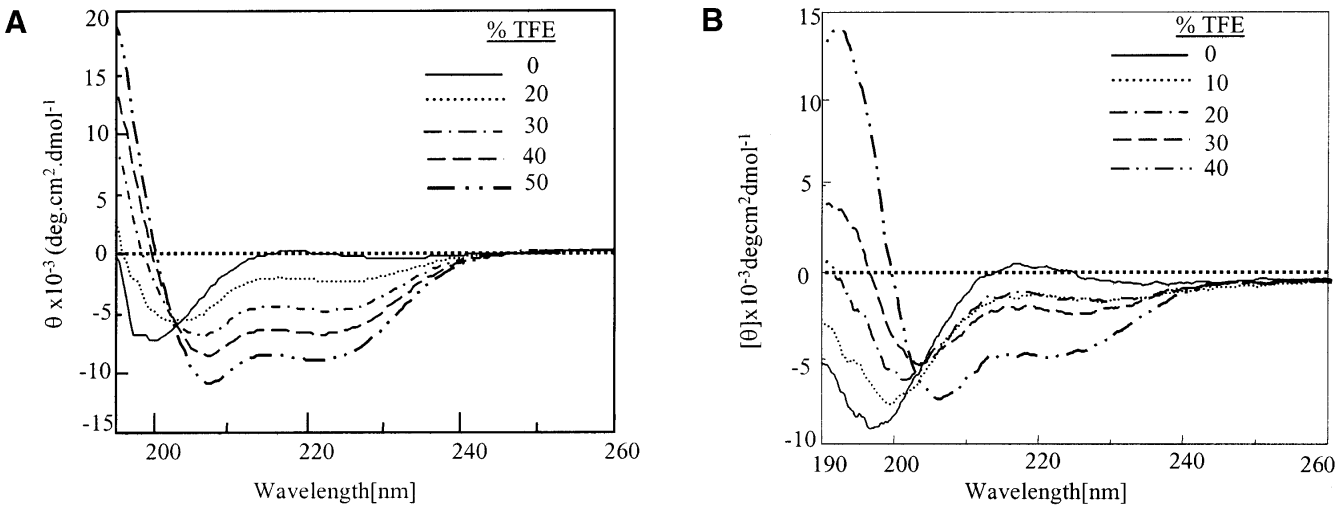

Figure 6. Effect of TFE on disaggregated (unordered) $Q_{12}HQHQ_{12}HQHQ_{12}$ and Q_8PQPQ_8. (*A*) Data indicate that $Q_{12}HQHQ_{12}HQHQ_{12}$ adopts sufficient helical character at 50% TFE (dot, dash line). (*B*) Q_8PQPQ_8 adopts sufficient helical conformation at 40% TFE concentration (dash, dash line) with a sharp minimum at 208 nm.

potential to retain the helical character for a longer period of time.

Acetonitrile, which has a β-stabilizing effect, also exerted some effect on the unordered peptide obtained after disaggregation (Barrow et al. 1992; Sonnichsen et al. 1992; Fabian et al. 1993; Otvos et al. 1993; El-Agnaf et al. 1998). All these peptides exhibited transition from random to β structure with an increase in acetonitrile concentration. Our findings suggest a higher tendency of polyglutamines without histidine interruptions to adopt a β structure. Q_{42} adopted β structure at the 35–45% range, whereas $Q_{12}HQHQ_{12}HQHQ_{12}$ adopted β conformation at a 60% acetonitrile concentration (data not shown). Figure 7 displays different conformations adopted by monomeric $Q_{12}HQHQ_{12}HQHQ_{12}$ under different solution conditions. These solvent systems were selected for this study considering their membrane mimicking nature in an aqueous environment. There is a possibility of such transitions even in the biological systems and their solubility or precipitation seemed to be governed to a very large extent by the prevailing solution conditions.

Structural transitions with temperature

The peptides under consideration in the β conformation (before TFA/HFIP disaggregation) when subjected to temperature-dependent study exhibited interesting results. Figure 8 demonstrates the thermal melting profile of $Q_{12}HQHQ_{12}HQHQ_{12}$ (Fig. 8A) and Q_{42} (Fig. 8B) in sodium chloride/sodium citrate buffer. The former displayed a decrease in intensity of both π–π* positive and n–π* negative bonds at 196 nm and 220 nm, respectively. The decrease in ellipticity was found to be more abrupt in the range of 45° to 65°C. The positive band seemed to shift progressively toward a lower wavelength, finally adopting a random structure with a negative band at 197 nm between 85° and 95°C indicating a complete collapse of the β structure. In comparison, Q_{42}, when subjected to similar conditions did not display transition from β structure to random and retained its β structure even at a temperature as high as 95°C, although there was a considerable loss of β-sheet content, as shown in Figure 8B. The positive band showed a dip but negative band at 222 nm displayed a marginal change on increasing the temperature. The temperature

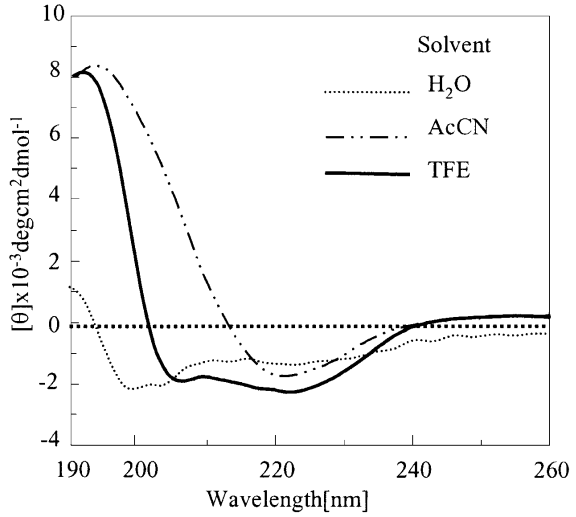

Figure 7. Solvent-dependent conformational transitions of $Q_{12}HQHQ_{12}HQHQ_{12}$ (disaggregated). In aqueous buffer the peptide displays an unordered structure (dotted line), presence of TFE results in an α helical (solid line), whereas acetonitrile provides a β conformation (dot, dash line).

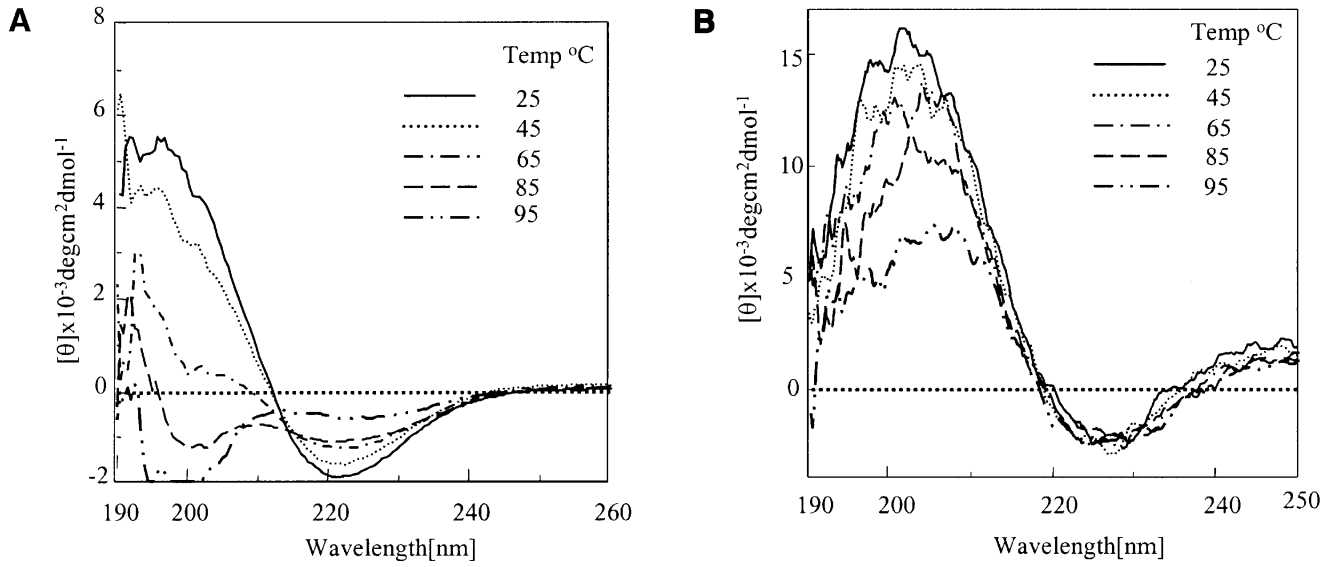

Figure 8. Temperature-dependent study of aggregated (β) $Q_{12}HQHQ_{12}HQHQ_{12}$ and Q_{42}. (*A*) $Q_{12}HQHQ_{12}HQHQ_{12}$ displays transition from β to an unordered conformation at 95°C (dot, dash line) and retains it over a longer period of time. (*B*) Q_{42} on the other hand retains its β structure even at 95°C (dot, dash line), although it displays a considerable loss of β-sheet content. The results suggest greater rigidity of β structure of Q_{42}.

range 85°–95°C displayed an abrupt decrease in ellipticity, indicating a major decrease in β-sheet content. $Q_{12}HQHQ_{12}HQHQ_{12}$ displayed a sharp isodichromic point at 210 nm (Fig. 8A; Cantor and Schimmel 1980); Q_{42}, on the other hand, did not display an isodichromic point (Fig. 8B) and retained its β conformation throughout. Even peptides with proline substitution underwent a similar transition from β to unordered conformation, displaying an isodichromic point at 210 nm.

The random peptide obtained after thermal denaturation (Fig. 8A), from all the histidine and proline interrupted peptides, when subjected to TFE titration indicated a transition from random to α helix, thus again displaying its α-helical propensity as observed in case of disaggregated (monomeric) peptides (Fig. 6). Denatured $Q_{12}HQHQ_{12}HQHQ_{12}$ left at room temperature for days displayed a slow transition to a β structure. The temperature and solvent-driven transitions observed in interrupted polyglutamines is illustrated schematically in Figure 9.

Solid phase FT-IR

The conformational analysis of all the peptides in solid phase was carried out by recording the second derivative FT-IR spectra in KBr. Figure 10 shows the FT-IR spectra of $Q_{12}HQHQ_{12}HQHQ_{12}$ obtained after lyophilization of the HPLC-purified peptide. The spectra displayed major amideI peaks at 1608, 1636, 1662, 1683, 1696 cm^{-1}, indicative of a β conformation (Byler and Susi 1986; Surewicz et al. 1990; Sharma et al. 1999). The bands at 1645 and 1652 cm^{-1} are mainly due to components of unordered and α-helical conformations.

Discussion

Studies using synthetic peptides as tools to identify structural changes in the local secondary structure of proteins upon sequence mutations and post-translational modifications have been reported by various groups of investigators. The conformation of polyglutamines, based on model peptides, has been discussed by different groups (Perutz et al. 1994; Altschuler et al. 1997; Kelly 1998; Sharma et al. 1999; Chen et al. 2001) and at present it is still an unresolved issue. Our present work on polyglutamines with and without interruptions suggests that polyglutamines are capable of exhibiting different conformations (Figs.1,3) and propensity for aggregation (Fig. 4) is governed not only by their repeat length but also is very much dependent on the nature of the sequence (interruptions). Our work also sug-

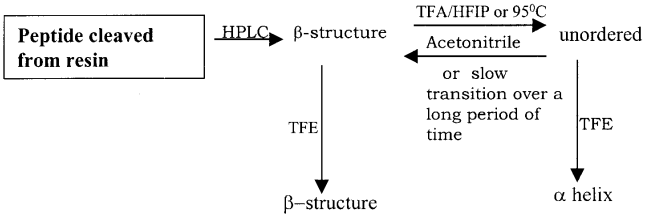

Figure 9. Various solvent and temperature driven conformational transitions observed in case of $Q_{12}HQHQ_{12}HQHQ_{12}$ indicating the conformational flexibility of the structure.

gests that adoption of β structure does not invariably lead to insolubility or immediate precipitation; peptides with histidine interruptions are capable of remaining in soluble aggregate form up to a higher concentration range and over a longer period of time. In addition, the present work reveals even greater solubility and lower propensity of β structure adoption (Table 1) of proline-containing model peptides as compared to histidine-interrupted ones.

The intramolecular nature of $Q_{12}HQHQ_{12}HQHQ_{12}$ in the β state is demonstrated by the concentration independent CD pattern as shown in Figure 1A. In contrast, the concentration-dependent CD profile (Fig.1B) of Q_{42} suggests a wide intermolecularly hydrogen bonded β-sheet structure. The intramolecular nature of $Q_{12}HQHQ_{12}HQHQ_{12}$ is further displayed by stabilization of the β structure in presence of TFE (Fig. 5). The stabilization of β conformation of interrupted peptides in presence of TFE (Blanco et al. 1994; Luo and Baldwin 1997) could possibly be justified by assuming a β hairpin-like structure as shown in Figure 11, as intramolecular hydrogen bonding also has a significant role in stabilizing such conformations. In comparison, Q_{42} has been found to be unaffected by TFE in the β state in the present study. This could possibly be attributed to the inherent property of TFE to reduce hydrophobic as well as neighborhood interactions between separate strands, which are considered to be immensely important for the stabilization of wide intermolecularly hydrogen-bonded β-sheet-rich structure (as suggested to be present in Q_{22} or Q_{42}).

The finding that TFE has a profound effect on all the disaggregated peptides (Fig. 6) adds support to our assumption that the disaggregated peptides are in a monomeric state. Futhermore, the fact that histidine and proline interrupted peptides adopt α-helical conformation with greater ease indicates their greater propensity for a helical structure as compared to continuous stretches. Also, the observation that uninterrupted peptides (in α helical state) left in TFE has a tendency for slow transition toward a β structure might suggest that helical conformation, in case of continuous stretch polyglutamines, is a temporary (unstable) state. Furthermore, our observation that continuous stretch pep-

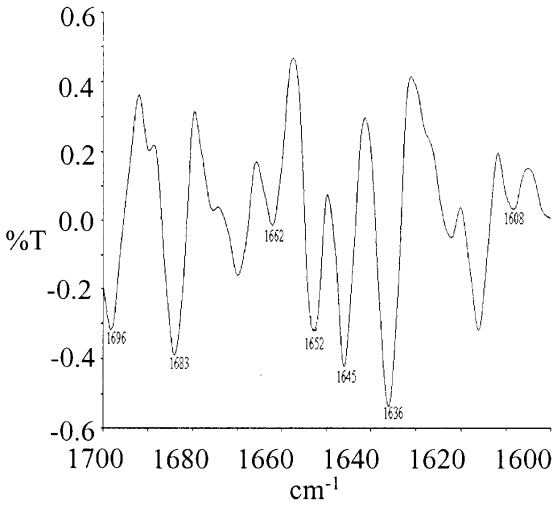

Figure 10. Second derivative FT-IR spectra of $Q_{12}HQHQ_{12}HQHQ_{12}$ in the solid state, peaks at 1608, 1636, 1662, 1683, 1696 cm^{-1} indicate a β conformation, whereas the bands at 1645 and 1652 $cm^{-1}$are possibly due to components of unordered and α-helical conformations.

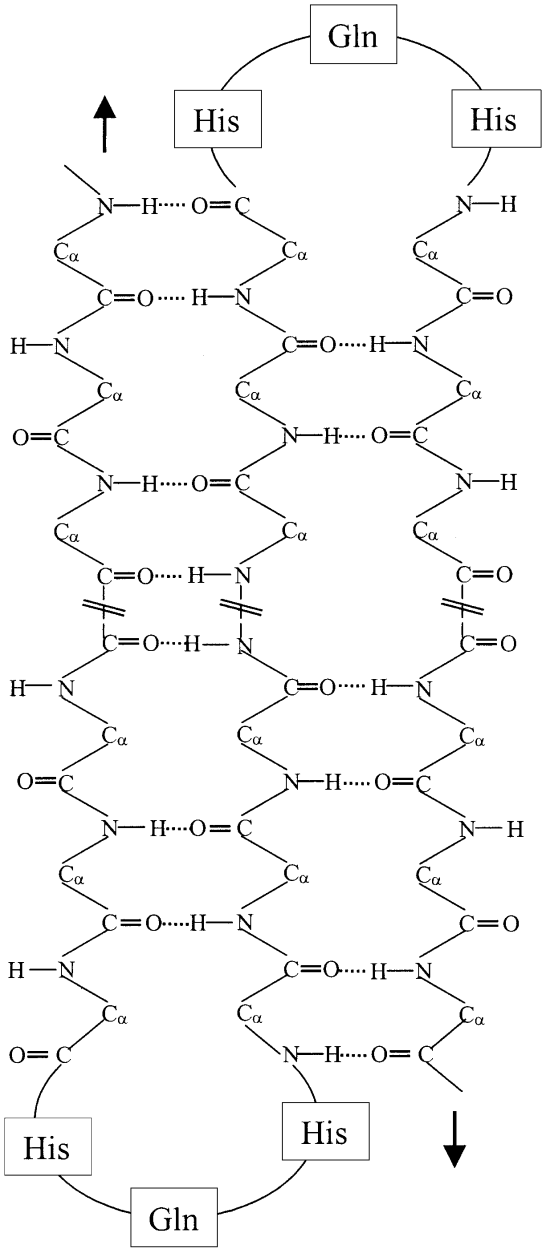

Figure 11. Proposed β structure of $Q_{12}HQHQ_{12}HQHQ_{12}$, which shows an intramolecularly hydrogen bonded β hairpin structure. The histidine interruption possibly brings about a fold in the structure, which restricts propagation of wide intermolecularly hydrogen-bonded β sheet, thus lowering the aggregation propensity.

tides adopt β structure with greater ease in presence of (β-stabilizing) acetonitrile adds support to our finding (Table 1) that they have a greater inherent tendency to adopt an extended β structure from an unordered conformation.

The temperature-dependent CD study also reveals the greater flexibility of the β structure of $Q_{12}HQHQ_{12}HQHQ_{12}$, which displays a clear transition from β to unordered conformation (Fig. 8A), whereas Q_{42} retains the stable β state even at 95°C (Fig. 8B). These structural characteristics could possibly be explained considering a β hairpin-type folded structure (Sharma et al. 1999) as shown in Figure 11. This type of structure encourages to bring together the hydrogen bonding entities of the same molecule to closer proximity, thus facilitating intramolecular hydrogen bonding to a greater extent as compared to interactions between neighboring entities (wide intermolecular hydrogen bonding). In the case of continuous stretch, because of high β-sheet forming propensity of glutamine (β-sheet forming potential trend Gln > His > Pro; Zhu and Braun 1999), the chain can progress without a fold in the structure. Thus, it can facilitate wide intermolecular hydrogen bonding, resulting in greater rigidity as displayed by the suggested structure of Q_{22} in our earlier work (Sharma et al. 1999). Hence, the biophysical characterization of the SCA1 peptides in the present work, lends support to the prediction that glutamine acts as a β-sheet promoter and histidine, a sheet breaker.

Our speculation of a turn at the HQH motif is further strengthened by a very similar behavior of proline-interrupted peptides, which is reported to have a significantly higher propensity for producing a turn in the structure (β turn potential trend is QPQP > QHQP > QHQH > QQQQ; Hutchinson and Thornton 1994; Guruprasad and Rajkumar 2000). The β-sheet inhibiting effect of proline incorporated sequences have been mainly attributed to the inefficiency of the proline ring to participate in the β-sheet H-bonding network (Wood et al. 1995). Although it is not justified to assign the exactly similar reasons to the greater solubility of histidine-incorporated poly Q sequences, it is likely that the ring structure of histidine has a role to play in destabilizing the intermolecularly hydrogen bonded wide β-sheet structure.

A comparison of the conformational properties of Q_{42} with $Q_{12}HQHQ_{12}HQHQ_{12}$ indicates that the former has greater potential to form a large intermolecular β-sheet structure through extended hydrogen bonding and thus greater aggregation potential. Histidine interruptions, on the other hand, in $Q_{12}HQHQ_{12}HQHQ_{12}$ restrict wide and rigid β-sheet formation and demonstrate a greater propensity for intramolecular hydrogen bonding. The greater solubility, relatively slow aggregation propensity of $Q_{12}HQHQ_{12}HQHQ_{12}$ compared not only to Q_{42} but even Q_{22} (which is of much shorter length and falls in the nonpathogenic range) could possibly explain why individuals (Quan et al. 1995; Calabresi et al. 2001) with such a long expansion ($Q_{12}HQHQ_{12}HQHQ_{14/15}$) were found to be phenotypically normal.

The peptide models developed in this study provide an insight into the understanding of the process of aggregation and conformational behavior of protein with long tracks of glutamine residues with and without interruptions. The conformation-dependent slow aggregation property observed in case of interrupted stretches, even in the disease range, might possibly suggest that at a very low concentration the protein aggregation in normal cells is either not initiated at all or the disease onset is significantly delayed.

Materials and methods

Peptide design and synthesis

Polyglutamine peptides with and without interruptions of varied length were designed and synthesized with the aim of studying their conformational properties. $Q_{12}HQHQ_{12}HQHQ_{12}$ was synthesized keeping in mind its biological relevance as discussed earlier and it was compared with uninterrupted Q_{42} of similar length at every stage. To examine the effect of length on conformational properties, Q_{22} and Q_8HQHQ_8 were studied at each stage. To ascertain whether any other amino acid of comparable structure, other than histidine, has a similar effect on solubility, proline was substituted to obtain Q_8HQPQ_8 and Q_8PQPQ_8.

The peptides $Q_{12}HQHQ_{12}HQHQ_{12}$, Q_{42}, Q_{22}, Q_8HQHQ_8, Q_8HQPQ_8, and Q_8PQPQ_8 were synthesized in-house using Wang-resin (batch method) on an advanced Chemtech Act 90 peptide synthesizer using standard protocols of F-moc chemistry. All the peptides were cleaved from resin using a mixture of TFA, phenol, and ethanedithiol and final purification was done on reverse phase using 70:30:water:acetonitrile and 0.05% TFA. The integrity of the peptide sequence was established by automated peptide sequencing (Procise 491, Applied Biosystems) and MALDI-ToF analysis (Kratos analytical).

Disaggregation of peptides using TFA/HFIP

HPLC-purified peptides were disaggregated following a recently reported method of disaggregation of polyglutamines (Chen et al. 2001). The peptides were suspended in a mixture of TFA and HFIP (1:1) and left at room temperature until it dissolved completely. The solvent mixture was removed under a stream of argon. The residue was dissolved in water adjusted at pH 3 with TFA. This was followed by ultracentrifugation to get rid of aggregates further. The peptides were stored at −70°C.

MALDI-ToF

All the peptides under study were subjected to MALDI-ToF analysis before and after the disaggregation step. Mass spectra were obtained on a KRATOS KOMPACT MALDI 4 Linear / Reflectron time of flight mass spectrometer, equipped with a pulsed nitrogen laser (337 nm). The instrument was operated in the linear, positive ion, high voltage (20 kv) mode. Spectra were acquired and processed using software provided by the manufacturer.

HPLC

The HPLC profile of all the peptides were studied before and after the disaggregation experiments on Waters 996 with photodiode array detector on reverse phase using mixtures of 70:30:water:acetonitrile and 0.05% TFA.

Rayleigh scattering

The peptides were subjected to Rayleigh scattering using JOBIN Yvon Horiba Fluorimax-3 fluorimeter. The emission and excitation wavelengths were both set at 450 nm and with the emission and excitation and slit widths both set at 2 nm.

CD

CD measurements were made on a Jasco J-715 spectropolarimeter with Peltier Thermo Controller (PTC). Spectra were recorded at a scan speed of 50 nm/min over the range of 190–260 nm in rectangular quartz cells of 0.1-, 0.5-, and 1-cm path length. All spectra were corrected by subtracting the baseline of the appropriate solvent and results are expressed as molar ellipticity [θ] in deg cm^2 $dmole^{-1}$. The spectra reported are an average of 8–12 scans. The peptide samples were previously dissolved in water and aliquots of the required amount were added to make samples of various concentrations of peptides in 3.3 mM sodium chloride/sodium citrate buffer at pH 7.2. Concentration of the peptide was determined by optical density measurement (OD) taken at 220 nm where the extinction coefficient is 624 m^{-1} cm^{-1}.

Solid-state FT-IR

FT-IR spectra were recorded on a Perkin Elmer spectrum 1000 FT-IR spectrometer at room temperature using KBr as medium. Deconvolution and second derivative analysis of the spectra were carried out using the software supplied by the manufacturer.

Acknowledgments

The research is supported by the grant provided by the Department of Biotechnology, Government of India, India. The publication costs of this article were defrayed in part by payment of page charges. This article must therefore be hereby marked "advertisement" in accordance with 18 USC section 1734 solely to indicate this fact.

References

Altschuler, E.L., Hud, N.V., Mazrimas, J.A., and Rupp, B. 1997. Random coil conformation for extended polyglutamine stretches in aqueous soluble monomeric peptides. *J. Pept. Res.* **50:** 73–75.

Barrow, C.J., Yasuda, A., Kenny, P.T., and Zagorski, M.G. 1992. Solution conformations and aggregational properties of synthetic amyloid β-peptides of Alzheimer's disease. *J. Mol. Biol.* **225:** 1075–1093.

Blanco, F., Jimenez, M.A., Pineda, A., Rico, M., Santoro, J., and Nieto, J.L. 1994. NMR solution structure of the isolated N-terminal fragment of protein-G B1 domain. Evidence of trifluoroethanol induced native-like β-hairpin formation. *Biochemistry* **33:** 6004–6014.

Brahmachari, S.K., Sharma, D., Sharma, S., Pasha, S., Sen, S., and Saleem, Q. 2000. Probing the polyglutamine puzzle in neurological disorders. *FEBS Lett.* **472:** 167–168.

Byler, D.M. and Susi, H. 1986. Examination of secondary structure of proteins by deconvolued FTIR spectra. *Biopolymers* **25:** 469–487.

Calabresi, V., Guida, S., Servadio, A., Fontali, M., and Jodice, C. 2001. Phenotypic effects of expanded ataxin-1 polyglutamines with interruptions *in vitro*. *Brain Res. Bull.* **56:** 337–342.

Cantor, C. and Schimmel, P. 1980. *Biophysical chemistry.* W H. Freeman & Co., San Francisco, CA.

Chen, S. and Wetzel, R. 2001. Solubilization and disaggregation of polyglutamine peptides. *Protein Sci.* **10:** 887–891.

Chen, S., Berthelier, V., Yang, W., and Wetzel, R. 2001. Polyglutamine aggregation behavior *in vitro* supports a recruitment mechanism of cytotoxicity. *J. Mol. Biol.* **31:** 173–182.

Chen, S., Berthelier, V., Hamilton, J.B., O'Nuallin, B., and Wetzel, R. 2002. Amyloid like features of polyglutamine aggregates and their assembly kinetics. *Biochemistry* **41:** 7391–7399.

Chothia, C. 1973. Conformation of β pleated sheets in proteins. *J. Mol. Biol.* **75:** 295–302.

Chung, M.Y., Ranum, L.P., Duvick, L.A., Servadio, A., Zoghbi, H.Y., and Orr, H.T. 1993. Evidence for a mechanism predisposing to intergenerational CAG repeat instability in spinocerebellar ataxia type I. *Nat. Genet.* **5:** 254–258.

Cummings, C.J. and Zoghbi, H.Y. 2000. Fourteen and counting: Unraveling trinucleotide repeat diseases. *Hum. Mol. Genet.* **9:** 909–916.

David, G., Abbas, N., Stevanin, G., Durr, A., Yvert, G., Cancel, G., Weber, C., Imbert, G., Saudou, F., Antoniou, E., et al. 1997. Cloning of the SCA7 gene reveals a highly unstable CAG repeat expansion. *Nat. Genet.* **17:** 65–70.

Davies, S.W., Turmaine, M., Cozens, B.A., DiFiglia, M., Sharp, A.H., Ross, C.A., Scherzinger, E., Wanker, E.E., Mangiarini, L., and Bates, G.P. 1997. Formation of neuronal intranuclear inclusions (NII) underlies the neurological dysfunction in mice transgenic for the HD mutation. *Cell* **90:** 537–548.

El-Agnaf, O.M.A., Bodles, A.M., Guthrie, D.J.S., Harriott, P., and Irvine, G.B. 1998. The N-terminal region of non-Aβ component of Alzheimer's disease amyloid responsible for its tendency to assume β-sheet and aggregate to form fibrils. *Eur. J. Biochem.* **258:** 157–163

Fabian, H., Szendrei, G.I., Mantsch, H.H., and Laszlo, Jr., O. 1993. Comparative analysis of Human and Dutch type alzheimer β-amyloid peptides by infrared spectroscopy and circular dichroism. *Biochem. Biophys. Res. Comm.* **191:** 232–239.

Greenfield, N. and Fasman, G.D. 1969. Computed circular dichroism spectra for the evaluation of protein conformation. *Biochemistry* **8:** 4108–4116.

Guruprasad, K. and Rajkumar, S. 2000. β and γ turns in proteins revisited: A new set of amino acid turn type dependent positional preferences and potentials. *J. Biosci.* **25:** 143–156.

Hutchinson, E.G. and Thornton, J.M. 1994. A revised set of potentials for β turn formation in proteins. *Protein Sci.* **3:** 2207–2216.

Kelly, J.W. 1998.The environmental dependency of protein folding best explains prion and amyloid diseases. *Proc. Natl. Acad. Sci.* **95:** 930–932.

Koo, E.H., Lansbury, Jr., P.T. and Kelly, J.W. 1999. Amyloid diseases: Abnormal protein aggregation in neurodegeneration. *Proc. Natl. Acad. Sci.* **96:** 9989–9990.

Luo, P. and Baldwin, R.L. 1997. Mechanism of helix induction by trifluoroethanol: A framework for helix forming properties of peptides from trifluoroethanol/water mixtures back to water. *Biochemistry* **36:** 8413–8421.

Martindale, D., Hackam, A., Wieczorek, A., Ellerby, L., Wellington, C., McCutcheon, K., Singaraja, R., Kazemi-Esfarjani, P., Devon, R., Kim, S.U., et al. 1998. Length of Huntington and its polyglutamine tract influences localization and frequency of intracellular aggregates. *Nat. Genet.* **18:** 150–154.

Nakamura, K., Jeong, S.Y., Uchihara, T., Anno, M., Nagashima, T., Ikeda, S., Tsuji, S., and Kanazawa, I. 2001. SCA17, a novel autosomal dominant cerebellar ataxia caused by an expanded polyglutamine in TATA-binding protein. *Hum. Mol. Genet.* **10:** 1441–1448.

Orr, H.T, Chung, M.Y., Banfi, S., Kwiatkowski, T.J., Servadio, A., Beaudet, A.L, McCall, A.E., Duvick, L.A., Ranum, L.P.W., and Zoghbi, H.Y. 1993. Expansion of an unstable trinucleotide CAG repeat in spinocerebellar ataxia type I, *Nat. Genet.* **4:** 221–226.

Otvos, Jr., L., Szendrei, G.I., Lee, V.M., and Mantsch, H.H. 1993. Human and rodent alzheimer β-amyloid peptides acquire conformation in membrane mimicking solvents. *Eur. J. Biochem.* **211:** 249–257.

Perutz, M.F., Johnson, T., Suzuki, M., and Finch, J.T. 1994. Glutamine repeats as polar zippers: Their possible role in inherited neurodegenerative diseases. *Proc. Natl. Acad. Sci.* **91:** 5355–5358.

Quan, F., Janas, J., and Popovich, B.W. 1995. A novel CAG repeat configuration in the SCA1 gene: Implications for the molecular diagnostics of spinocerebellar ataxia type 1. *Hum. Mol. Genet.* **4:** 2411–2413.

Sharma, D., Sharma, S., Pasha, S., and Brahmachari, S.K., 1999. Peptide models for inherited neurodegenerative disorders: Conformation and aggregation properties of long polyglutamine peptides with and without interruptions. *FEBS Lett.* **456:** 181–185.

Sonnichsen, F.D., Van Eyk, J.E., Hodges, R.S., and Sykes, B.D. 1992. Effect of trifluoroethanol on protein secondary structure: An NMR and CD study using a synthetic actin peptide. *Biochemistry* **31:** 8790–8798.

Surewicz, W.K., Leddy, J.J., and Mantsch, H.H. 1990. Structure, stability and receptor interaction of cholera toxin as studied by Fourier transform infrared spectroscopy. *Biochemistry* **29:** 8106–8111.

Wood, S.J., Wetzel, R., Martin, J.D., and Hurle, M.R. 1995. Prolines and amyloidogenecity in fragments of the Alzheimer's peptide β/A4. *Biochemistry* **34:** 724–730.

Woody, R.W. 1995. Circular dichroism. *Methods Enzymol.* **246:** 34–71.

Zhu, H. and Braun, W. 1999. Sequence specificity, statistical potentials, and three-dimensional structure prediction with self-correcting distance geometry calculations of β-sheet formation in proteins. *Protein Sci.* **8:** 326–342.